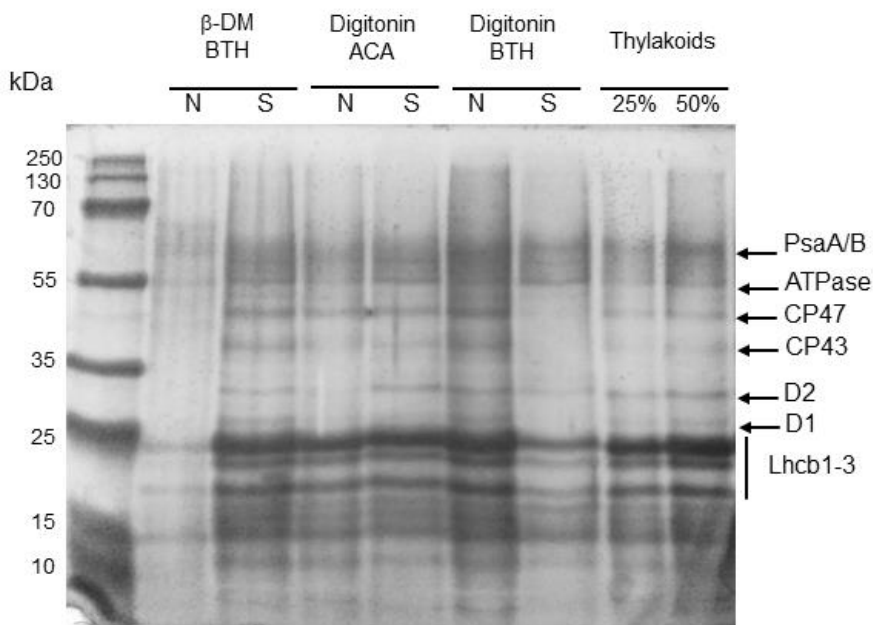


## Thylakoid membrane appressions in the giant chloroplast of *Selaginella martensii* Spring: a lycophyte challenges grana paradigms in shade-adapted species

Andrea Colpo, Alessandra Molinari, Paola Boldrini, Marek Živčák, Marian Breštič, Sara Demaria, Costanza Baldisserotto, Simonetta Pancaldi, Lorenzo Ferroni

### SUPPLEMENTARY MATERIAL

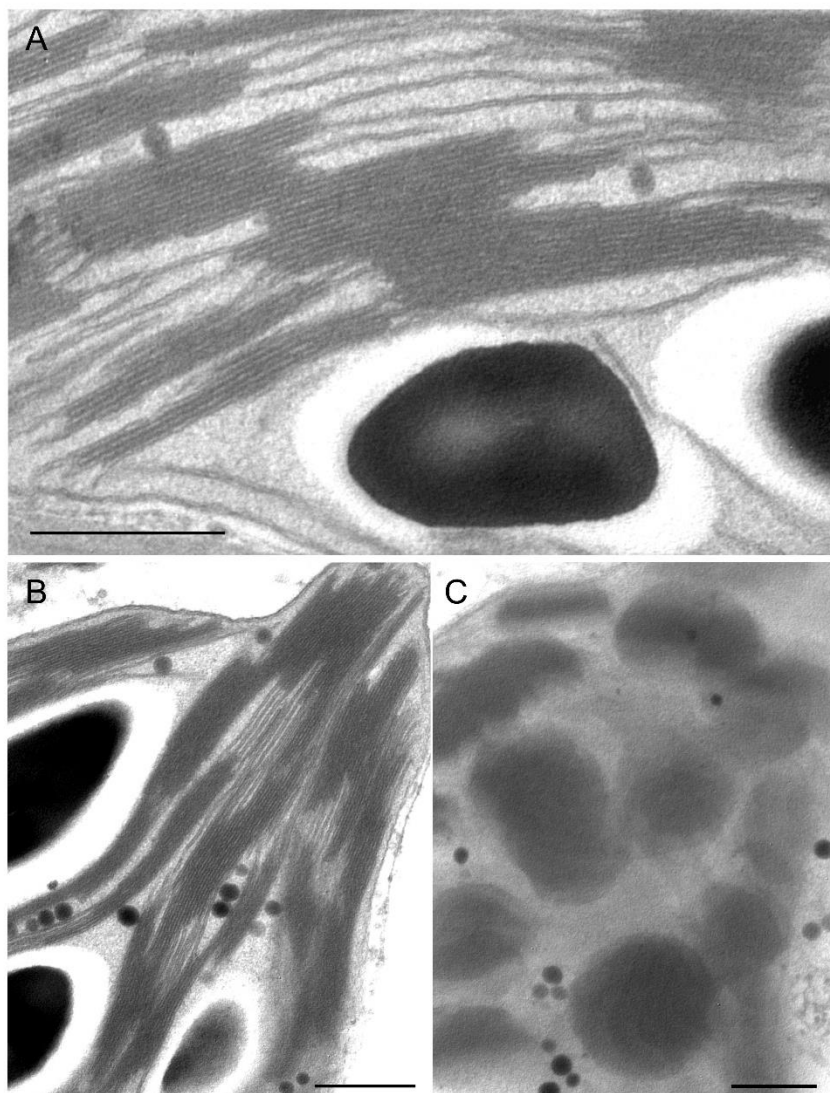


**Supplementary Figure S1.** Proteins of the thylakoid membranes of *Selaginella martensii* solubilized with different detergents and subsequently separated on denaturing SDS-PAGE.

Thylakoid membranes corresponding to 8 µg chlorophyll were solubilized with 1.5% β-dodecyl maltoside (β-DM) in bis-tris-HCl (BTH) buffer, or 1.5% digitonin in BTH, or 1.5% digitonin in aminocaproic acid buffer (ACA) and, after centrifugation, the solubilized (supernatant) and non-solubilized (pellet) were separated (see paragraph 2.4 of the main text). Subsequently, 15 µL of 2× Laemmli buffer (Laemmli 1970) was added to all samples with the necessary volume of deionized water to reach a total sample volume of 30 µL. After vigorous vortexing, the samples were incubated for 15 min at 60°C to promote protein denaturation. After centrifugation at 18.000 g for 5 min, the supernatant was recovered and loaded into the gel for the electrophoretic run according to routine protocols. For reference, entire thylakoids were denatured using the same protocol and loaded in the same gel. Bands were silver stained, and the proteins were assigned based on Ferroni et al. (2014, 2016): PsaA/B, core proteins of PSI reaction centre; ATPase, ATP-β subunit of the ATP synthase; CP47 and CP43, proteins PsbC and PsbB of the inner antenna complexes of PSII core, respectively; D1 and D2, core

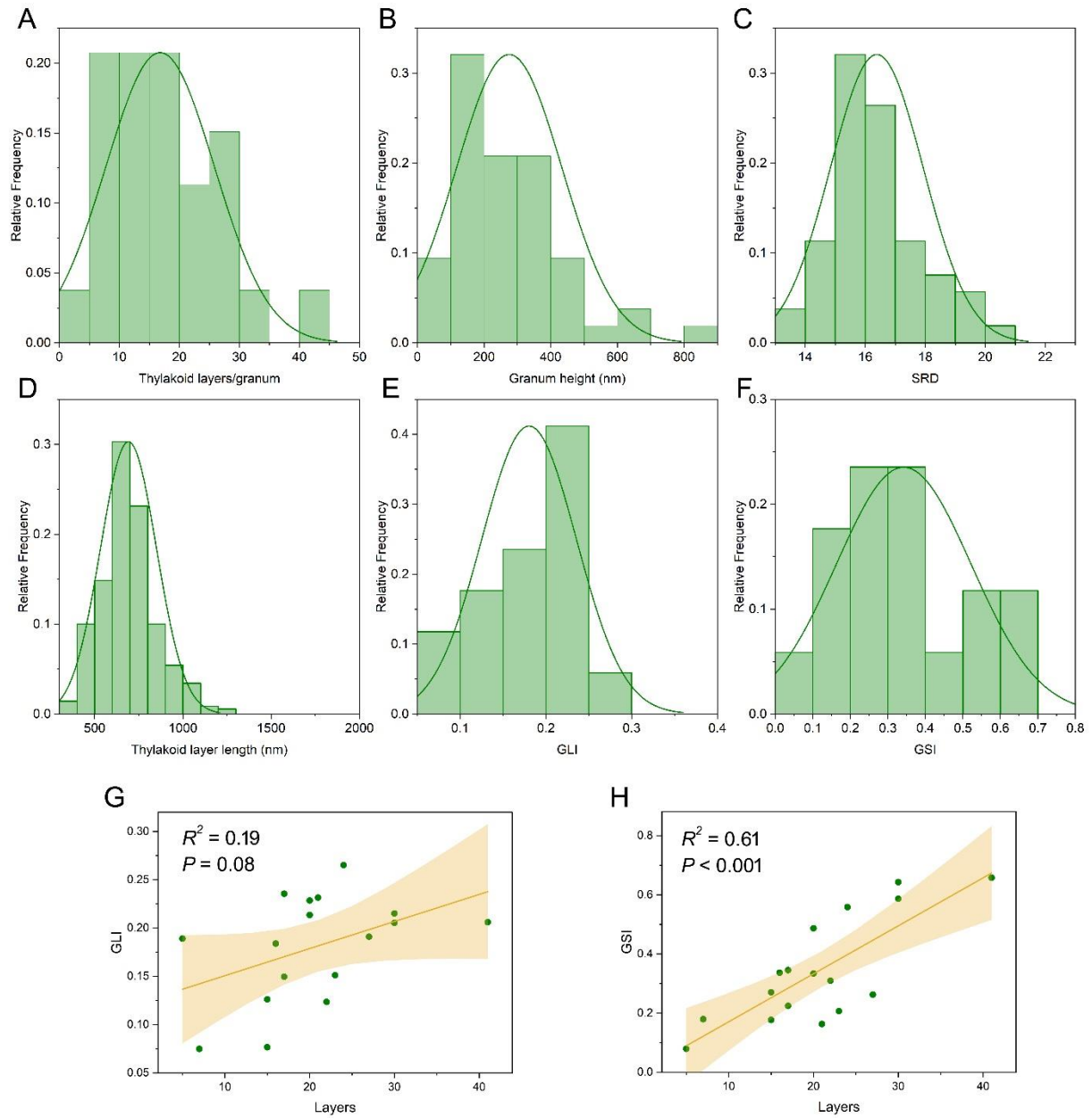
proteins of the PSII reaction centre; LhcB1-3, subunits of the major light-harvesting complex of PSII, LHCII. N, detergent-insoluble fraction; S, detergent-soluble fraction.

Note that the insoluble fraction after digitonin-BTH treatment still contains PsaA/B and ATP- $\beta$ , which are typically excluded from the grana cores because their steric hindrance at the stromatic side, meaning that the insoluble fraction also includes some stroma-exposed membranes. After digitonin-ACA treatment, the evident D2 enrichment in the soluble fraction, without a similar enrichment in the other PSII subunits, is indicative of an artifact occurred during the solubilization.



**Supplementary Figure S2.** Electron micrographs of the thylakoid system in the chloroplasts of the mesophyll and lower epidermis cells in *Selaginella martensii* leaf at the end of the night.

(A) Thylakoid system in a chloroplast hosted in a mesophyll cell. Note the co-existence of small grana formed by 4-6 layers and a large granum with a high degree of layer and cross-sectional irregularity. (B) The thylakoid system in a chloroplast of the lower epidermis exemplifies the occurrence of very wide granum layers. (C) In a chloroplast of the lower epidermal cell, a section tangent to the grana stacks shows individual disks with a large diameter and partly overlapping each other. Scale bars: 0.5  $\mu\text{m}$ .



Parameter	Upper epidermis	Mesophyll	<i>P</i> ( <i>df</i> )	Weighted mean
Thylakoid layers/granum	$15.1 \pm 0.7$	$16.8 \pm 1.2$	0.21 (185)	15.3
Granum height (nm)	$252.4 \pm 10.5$	$278.7 \pm 21.7$	0.28 (185)	255.6
SRD (nm)	$16.9 \pm 0.14$	$16.4 \pm 0.2$	<b>0.04 (185)</b>	16.8
Thylakoid layer length (nm)	$732.6 \pm 7.0$	$691.6 \pm 8.5$	<b>0.0011 (1280)</b>	727.6
GLI	$0.213 \pm 0.013$	$0.180 \pm 0.013$	0.14 (60)	0.209
GSI	$0.318 \pm 0.027$	$0.343 \pm 0.044$	0.63 (60)	0.321

**Supplementary Figure S3.** Granum morphometrics of the mesophyll chloroplasts of *Selaginella martensii* leaf.

(A) Height of the grana stacks. (B) Number of thylakoid layers per granum. (C) Stacking repeat distance, *SRD*. (D) Length of the thylakoid layers. (E) Granum lateral irregularity, *GLI*. (F) Granum cross-sectional irregularity, *GSI*. Histograms of the parameters, each reported with the corresponding normal distribution (for A, B, C,  $N=53$  grana; for D,  $N=350$  layers; for E and F,  $N=17$  chloroplasts. Morphometry was performed on 10 micrographs taken from 4 independent plants). (G-H) Co-variation of the number of thylakoid layers per

gratum with GLI or GSI. The regression lines with 95% confidence bands,  $R^2$  and corresponding  $P$  values are reported. For the definitions of parameters, see Mazur et al. (2020) and the main text of this paper, section 2.6.

The table reports grana morphometric parameters in comparison between the upper epidermis and mesophyll chloroplasts, with  $P$  values obtained using a Student's  $t$ -test. Degrees of freedom for each test ( $df$ ) are reported for each comparison. The weighted mean of the parameters is based on the estimates of the leaf area section covered by plastids belonging to the two tissues. The contribution by the lower epidermis chloroplasts is assumed to be negligible.

### Supplementary Table S1

Comparative values of the granum diameters in species of vascular plant. In some cases, the values are average diameters explicitly reported by the referenced papers, in others they were reckoned from published micrographs.

The reported values are affected by different methods and equipment used by laboratories for 50 years and are intended to give a rough idea about variation in granum width among vascular plants.

Plant species	Granum diameter (nm)	Reference
<b>Angiosperms Eudicots</b>		
<i>Arabidopsis thaliana</i>	410-470	Fristed et al. 2009 Armbruster et al. 2013
<i>Raphanus sativus</i>	536	Meier and Lichtenhaler 1981
<i>Lactuca sativa</i>	450-500	Kaftan et al. 2002
<i>Urtica dioica</i>	400-420	Pfeiffer and Krupinska 2005a
<i>Spinacia oleracea</i>	350-600	Daum et al. 2010 Kouril et al. 2011 Wood et al. 2019
<i>Fagus sylvatica</i>	339-399	Lichtenhaler et al. 1981
<i>Solanum lycopersicum</i>	390-430	Moriwaki et al. 2019
<i>Glechoma longituba</i> (shade)	430	Zhang et al. 2015
<i>Primulina tabacum</i> (shade)	550	Liang et al. 2011
<i>Panax quinquefolium</i> (deep shade)	400	Lee et al. 2017
<b>Angiosperms Monocots</b>		
<i>Hordeum vulgare</i>	480	Pfeiffer and Krupinska 2005b
<i>Hydrocharis morsus-ranae</i>	340	Kordyum et al. 2022
<i>Arum italicum</i> (shade)	470	Pancaldi et al. 1998
<i>Tradescantia albiflora</i> (deep shade)	530	Adamson et al. 1991
<i>Alocasia macrorrhiza</i> (deep shade)	483	Anderson et al. 1973 Chow et al. 1988
<i>Monstera deliciosa</i> (deep shade)	430	Demmig-Adams et al. 2015
<i>Anoectochilus roxburghii</i> (deep shade)	507-580	Shao et al. 2014
<b>Cycadophyte</b>		
<i>Lepidozamia peroffskyana</i> (shade)	450	Medeghini Bonatti and Fornasiero Baroni 1990
<b>Monilophytes (ferns)</b>		
<i>Acrostichum danaeifolium</i>	430	Fonini et al. 2017
<i>Asplenium australasicum</i> (deep shade)	726	Leong et al. 1985
<i>Trichomanes speciosum</i> (deep shade)	560	Makgomol and Sheffield 2001
<i>Teratophyllum rotundifoliatum</i> (deep shade)	1290	Nasrulhaq-Boyce and Duckett 1991
<b>Lycophytes</b>		
<i>Selaginella martensii</i>		
Giant chloroplast	733	
Mesophyll chloroplast	692	This report
<i>Selaginella erythropus</i>		
Giant chloroplast	594 - 680	Sheue et al. 2007, Ghaffar et al. 2018
Mesophyll chloroplast	662	Sheue et al. 2007
<i>Selaginella apoda</i>	660	Jagels 1970
<i>Isoetes sinensis</i>	860	Ding et al. 2015

## Supplementary Table S2

Thylakoid layers per granum  $N$  and granum regularity indexes in shade or deep-shade vascular plants (Granum lateral irregularity,  $GLI$ , and Granum cross-sectional irregularity,  $GSI$ ).  $N$  values are either declared in the referenced papers, or counted from the published micrographs or, when impossible to count, estimated by dividing the granum height by a postulated stacking repeat distance of 17 nm.  $GLI$  and  $GSI$  are estimated from micrographs published in the referenced papers.  $GI_{TOT}$  is the sum of  $GLI$  and  $GSI$ .

The reported values are affected by different methods and equipment used by laboratories for 50 years and are intended to give a rough idea about variation in granum regularity in vascular plants. Note that  $GSI$  is *negative* when the granum shape is convex (e.g., oval-like as in *Anoectochilus roxburghii*): in such cases, the granum is considered free of lateral sliding and a value of 0  $GSI$  was assigned.

<b>Plant species</b>	<b><i>N</i></b>	<b><i>GLI</i></b>	<b><i>GSI</i></b>	<b><i>GI<sub>TOT</sub></i></b>	<b>Reference</b>
<b>Angiosperms Eudicots</b>					
<i>Glechoma longituba</i>	19	0.17	0.19	0.36	Zhang et al. 2015
<i>Primulina tabacum</i>	17	0.15	0.05	0.20	Liang et al. 2011
<i>Panax quinquefolium</i>	21	0.18	0.11	0.29	Lee et al. 2017
<b>Angiosperms Monocots</b>					
<i>Arum italicum</i>	12	0.16	0.17	0.33	Pancaldi et al. 1998
<i>Tradescantia albiflora</i>	14	0.18	0.13	0.31	Adamson et al. 1991
<i>Alocasia macrorrhiza</i>	43 (max >100)	0.19	0.02	0.21	Anderson et al. 1973 Chow et al. 1988
<i>Monstera deliciosa</i>	53	0.09	0.33	0.42	Demmig-Adams et al. 2015
<i>Anoectochilus roxburghii</i>					Shao et al. 2014
20% sunlight	18	0.15	0.20	0.35	
5% sunlight	110	0.18	0	0.18	
<b>Cycadophyte</b>					
<i>Lepidozamia peroffskyana</i>	34 (max 120)	0.11	0.08	0.19	Medeghini Bonatti and Fornasiero Baroni 1990
<b>Monilophyta (ferns)</b>					
<i>Acrosticum danaeifolium</i>	9	0.16	0.10	0.26	Fonini et al. 2017
<i>Asplenium australasicum</i> (deep shade)	16	0.14	0.18	0.32	Leong et al. 1985
<i>Trichomanes speciosum</i> (deep shade)	18	0.16	0.18	0.34	Makgomol and Sheffield 2001
<i>Teratophyllum rotundifoliatum</i> (deep shade)	86 (max 280)	0.20	0.10	0.30	Nasrulhaq-Boyce and Duckett 1991
<b>Lycophtyes</b>					
<i>Selaginella martensii</i>					
Giant chloroplast	15 (max 48)	0.18	0.32	0.50	This report
Mesophyll chloroplast	17 (max 41)	0.21	0.34	0.55	
<i>Selaginella erythropus</i>	18 (max 44)	0.27	0.31	0.58	Sheue et al. 2007 Ghaffar et al. 2018
<i>Selaginella apoda</i>	13 (max 25)	0.19	0.22	0.41	Jagels 1970
<i>Isoetes sinensis</i>	8 (max 23)	0.17	0.06	0.23	Ding et al. 2015

## References

- Adamson, H. Y., Chow, W. S., Anderson, J. M., Vesk, M., & Sutherland, M. W. (1991). Photosynthetic acclimation of *Tradescantia albiflora* to growth irradiance: morphological, ultrastructural and growth responses. *Physiologia Plantarum*, 82(3), 353-359.
- Anderson, J. M., Goodchild, D. J., & Boardman, N. K. (1973). Composition of the photosystems and chloroplast structure in extreme shade plants. *Biochimica et Biophysica Acta (BBA)-Bioenergetics*, 325(3), 573-585.
- Armbruster, U., Labs, M., Pribil, M., Viola, S., Xu, W., Scharfenberg, M., et al. (2013). *Arabidopsis* CURVATURE THYLAKOID1 proteins modify thylakoid architecture by inducing membrane curvature. *The Plant Cell*, 25(7), 2661-2678.
- Chow, W. S., Qian, L., Goodchild, D. J., & Anderson, J. M. (1988). Photosynthetic acclimation of *Alocasia macrorrhiza* (L.) G. Don. *Functional Plant Biology*, 15(2), 107-122.
- Daum, B., Nicastro, D., Austin, J., McIntosh, J. R., & Kühlbrandt, W. (2010). Arrangement of photosystem II and ATP synthase in chloroplast membranes of spinach and pea. *The Plant Cell*, 22(4), 1299-1312.
- Demmig-Adams, B., Muller, O., Stewart, J. J., Cohu, C. M., & Adams III, W. W. (2015). Chloroplast thylakoid structure in evergreen leaves employing strong thermal energy dissipation. *Journal of Photochemistry and Photobiology B: Biology*, 152, 357-366.
- Ding, G., Li, C., Han, X., Chi, C., Zhang, D., & Liu, B. (2015). Effects of lead on ultrastructure of *Isoetes sinensis* Palmer (Isoetaceae), a critically endangered species in China. *PloS one*, 10(9), e0139231.
- Ferroni, L., Angelieri, M., Pantaleoni, L., Pagliano, C., Longoni, P., Marsano, F., et al. (2014). Light-dependent reversible phosphorylation of the minor photosystem II antenna Lhc6 (CP 24) occurs in lycophytes. *The Plant Journal*, 77(6), 893-905.
- Ferroni, L., Suorsa, M., Aro, E. M., Baldissерotto, C., & Pancaldi, S. (2016). Light acclimation in the lycophyte *Selaginella martensii* depends on changes in the amount of photosystems and on the flexibility of the light-harvesting complex II antenna association with both photosystems. *New Phytologist*, 211(2), 554-568.
- Fonini, A. M., Barufi, J. B., Schmidt, E. C., Rodrigues, A. C., & Randi, A. M. (2017). Leaf anatomy and photosynthetic efficiency of *Acrostichum danaeifolium* after UV radiation. *Photosynthetica*, 55(3), 401-410.
- Fristedt, R., Willig, A., Granath, P., Crevecoeur, M., Rochaix, J. D., & Vener, A. V. (2009). Phosphorylation of photosystem II controls functional macroscopic folding of photosynthetic membranes in *Arabidopsis*. *The Plant Cell*, 21(12), 3950-3964.

- Ghaffar, R., Weidinger, M., Mähnert, B., Schagerl, M., & Lichtscheidl, I. (2018). Adaptive responses of mature giant chloroplasts in the deep-shade lycopod *Selaginella erythropus* to prolonged light and dark periods. *Plant, Cell and Environment*, 41(8), 1791-1805.
- Jagels, R. (1970). Photosynthetic apparatus in *Selaginella*. II. Changes in plastid ultrastructure and pigment content under different light and temperature regimes. *Canadian Journal of Botany*, 48(10), 1853-1860.
- Kaftan, D., Brumfeld, V., Nevo, R., Scherz, A., & Reich, Z. (2002). From chloroplasts to photosystems: in situ scanning force microscopy on intact thylakoid membranes. *The EMBO journal*, 21(22), 6146-6153.
- Kordyum, E., Polishchuk, O., Akimov, Y., & Brykov, V. (2022). Photosynthetic Aaparatus of *Hydrocharis morsus-ranae* in different solar lighting. *Plants*, 11(19), 2658.
- Kouřil, R., Oostergetel, G. T., & Boekema, E. J. (2011). Fine structure of granal thylakoid membrane organization using cryo electron tomography. *Biochimica et Biophysica Acta (BBA)-Bioenergetics*, 1807(3), 368-374.
- Laemmli, U. K. (1970). Cleavage of structural proteins during the assembly of the head of bacteriophage T4. *Nature*, 227(5259), 680-685.
- Lee, O. R., Nguyen, N. Q., Lee, K. H., Kim, Y. C., & Seo, J. (2017). Cytohistological study of the leaf structures of *Panax ginseng* Meyer and *Panax quinquefolius* L. *Journal of Ginseng Research*, 41(4), 463-468.
- Leong, T. Y., Goodchild, D. J., & Anderson, J. M. (1985). Effect of light quality on the composition, function, and structure of photosynthetic thylakoid membranes of *Asplenium australasicum* (Sm.) Hook. *Plant Physiology*, 78(3), 561-567.
- Liang, K. M., Lin, Z. F., Ren, H., Liu, N., Zhang, Q. M., Wang, J., et al. (2010). Characteristics of sun-and shade-adapted populations of an endangered plant *Primulina tabacum* Hance. *Photosynthetica*, 48, 494-506.
- Lichtenthaler, H. K., C. Buschmann, M. Döll, H-J. Fietz, T. Bach, U. Kozel, D. Meier, & U. Rahmsdorf. (1981). Photosynthetic activity, chloroplast ultrastructure, and leaf characteristics of high-light and low-light plants and of sun and shade leaves. *Photosynthesis research*, 2, 115-141.
- Makgomol, K., & Sheffield, E. (2001). Gametophyte morphology and ultrastructure of the extremely deep shade fern, *Trichomanes speciosum*. *New Phytologist*, 151(1), 243-255.
- Mazur, R., Mostowska, A., & Kowalewska, Ł. (2021). How to measure grana—ultrastructural features of thylakoid membranes of plant chloroplasts. *Frontiers in Plant Science*, 12.
- Medeghini Bonatti, P. & Fornasiero Baroni, R. (1990) Developmental pattern and structural organisation of leaf chloroplasts in *Lepidozamia peroffskyana*. *Australian Journal of Botany*, 38, 53-62.
- Meier, D., & H. K. Lichtenthaler. (1981) Ultrastructural development of chloroplasts in radish seedlings grown at high-and low-light conditions and in the presence of the herbicide bentazon. *Protoplasma* 107: 195-207.

- Moriwaki, T., Falcioni, R., Tanaka, F. A. O., Cardoso, K. A. K., Souza, L. A., Benedito, E., et al. (2019). Nitrogen-improved photosynthesis quantum yield is driven by increased thylakoid density, enhancing green light absorption. *Plant Science*, 278, 1-11.
- Nasrulhaq-Boyce, A., & Duckett J. G. (1991) Dimorphic epidermal cell chloroplasts in the mesophyll-less leaves of an extreme-shade tropical fern, *Teratophyllum rotundifoliatum* (R. Bonap.) Holtt.: a light and electron microscope study. *New Phytologist* 119, 433-444.
- Pancaldi, S., Bonora, A., Gualandri, R., Gerdol, R., Manservigi, R., & Fasulo, M. P. (1998). Intra-tissue characteristics of chloroplasts in the lamina and petiole of mature winter leaf of *Arum italicum* Miller. *Botanica acta*, 111(4), 261-272.
- Pfeiffer, S., & Krupinska, K. (2005a). Chloroplast ultrastructure in leaves of *Urtica dioica* L. analyzed after high-pressure freezing and freeze-substitution and compared with conventional fixation followed by room temperature dehydration. *Microscopy research and technique*, 68(6), 368-376.
- Pfeiffer, S., & Krupinska, K. (2005b) New insights in thylakoid membrane organization. *Plant and Cell Physiology*, 46, 1443–1451
- Shao, Q., Wang, H., Guo, H., Zhou, A., Huang, Y., Sun, Y., & Li, M. (2014). Effects of shade treatments on photosynthetic characteristics, chloroplast ultrastructure, and physiology of *Anoectochilus roxburghii*. *PLoS One*, 9(2), e85996.
- Sheue, C. R., Sarafis, V., Kiew, R., Liu, H. Y., Salino, A., Kuo-Huang, L. L., et al. (2007). Bizonoplast, a unique chloroplast in the epidermal cells of microphylls in the shade plant *Selaginella erythropus* (Selaginellaceae). *American Journal of Botany*, 94(12), 1922-1929.
- Wood, W. H., Barnett, S. F., Flannery, S., Hunter, C. N., & Johnson, M. P. (2019). Dynamic thylakoid stacking is regulated by LHCII phosphorylation but not its interaction with PSI. *Plant Physiology*, 180(4), 2152-2166.
- Zhang, L. X., Guo, Q. S., Chang, Q. S., Zhu, Z. B., Liu, L., & Chen, Y. H. (2015). Chloroplast ultrastructure, photosynthesis and accumulation of secondary metabolites in *Glechoma longituba* in response to irradiance. *Photosynthetica* 53, 144-153.